

# High-Efficient Self-Excited Brushless Wound Rotor Synchronous Machine Topology

Syed Sabir Hussain Bukhari<sup>1b</sup> and Paavo Rasilo<sup>1b</sup>

Electrical Engineering Unit, Tampere University, 33720 Tampere, Finland

This article proposes a new armature winding configuration to implement the sub-harmonic field excitation method for brushless operation in wound rotor synchronous machines (WRSMs). The proposed configuration combines single- and double-layer winding arrangements to generate a fundamental and suitable magnitude of sub-harmonic magnetomotive force (MMF) components in the machine's air gap. The fundamental MMF creates the main stator field, while the sub-harmonic MMF component induces a harmonic current in the rotor's harmonic winding. This current is rectified through a serially connected full-bridge diode rectifier, which excites the rotor field winding to achieve brushless operation. The proposed brushless WRSM topology is validated using a 2-D finite element analysis (FEA), for an eight-pole, 48-slot machine model developed in JMAG-Designer version 22.2. Its performance is compared to that of a conventional dual-armature winding-based brushless WRSM topology. Results show that the proposed brushless WRSM topology achieves lower torque ripple, reduced losses, and higher efficiency than the conventional topology due to its single-winding configuration.

**Index Terms**—Brushless operation, sub-harmonic field excitation, synchronous machines, wound field machines.

## I. INTRODUCTION

IN RECENT years, wound rotor synchronous machines (WRSMs) have attracted considerable attention due to the absence of costly permanent magnets for their rotor field excitation [1], [2], [3]. To take advantage of the adjustable rotor field, the wound field synchronous machines have been used at the expense of repeated maintenance due to brushes and slip rings [2]. An extended-shaft arrangement is required for the exciters and pilot exciters, to energize the rotor field winding in a brushless synchronous machine [4]. However, this arrangement cannot be used in a scaled-down application such as an electric vehicle where the volume of the machine cannot exceed a certain limit. To make a compact brushless wound field synchronous machine an embedded excited or harmonic excitation system needs to be investigated [5].

The harmonically excited brushless WRSM topologies operate by developing an additional harmonic field along with the fundamental one, which induces current in an additional rotor winding. This winding is connected in series with the rotor field winding through a full-bridge diode rectifier [6]. The rotor structure in these topologies depends on the order of the harmonic field developed in the machine's air gap. In [7], a brushless WFSM based on the control of harmonic excitation current in the stator windings was proposed. The control of the harmonic excitation current generates a third-harmonic field in the machine's air gap. A harmonic current excited brushless WFSM based on an open winding configuration was introduced in [8] and [9]. These topologies require a dual-inverter configuration to generate a third-harmonic field in the machine. In [10], a brushless WFSM based on semi-open stator winding was proposed. The inverter configuration in this topology requires a higher number of power electronic switches to generate both the fundamental and third-harmonic fields.

Received 8 November 2024; revised 2 February 2025; accepted 16 March 2025. Date of publication 19 March 2025; date of current version 27 August 2025. Corresponding author: S. S. H. Bukhari (e-mail: syed.bukhari@tuni.fi).

Color versions of one or more figures in this article are available at <https://doi.org/10.1109/TMAG.2025.3552981>.

Digital Object Identifier 10.1109/TMAG.2025.3552981

© 2025 The Authors. This work is licensed under a Creative Commons Attribution 4.0 License. For more information, see <https://creativecommons.org/licenses/by/4.0/>

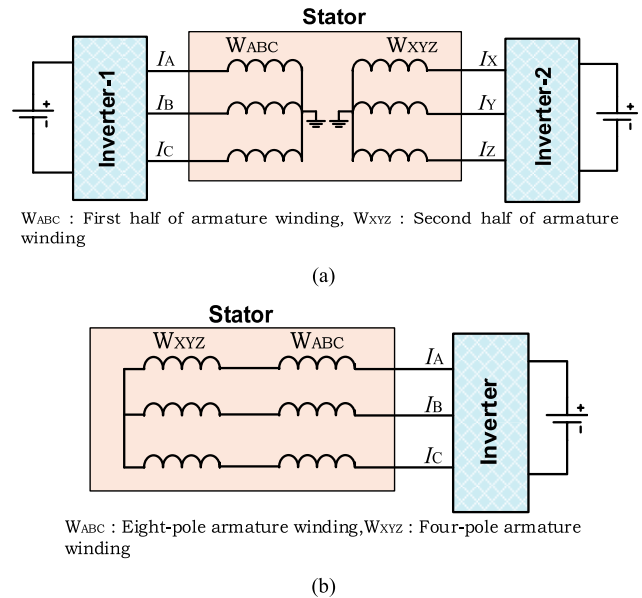


Fig. 1. Conventional sub-harmonic-based brushless WRSM topologies proposed in (a) [13] and (b) [14].

Similarly, in [11], a brushless WFSM with a double harmonic stator winding was introduced. In this topology, one winding generates the third harmonic field, while the second winding is responsible for producing the fundamental rotating field. A double third-harmonic current excitation principle for the brushless operation of a WFSM is proposed [12]. In this topology, two three-phase windings share a common star point. One winding is powered by an inverter with six switches, while the other is powered by an inverter with eight switches to generate both fundamental and third-harmonic fields.

The rotor structure in these topologies requires three times the harmonic winding poles to be placed on the rotor periphery. Low-order harmonic fields enable a simplified rotor structure, whereas high-order harmonic fields require a more complex rotor design to achieve brushless operation.



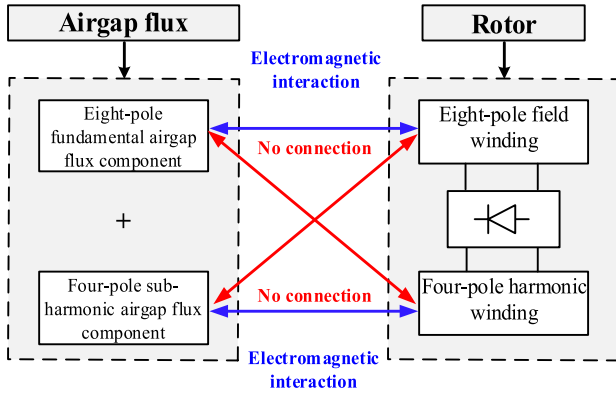


Fig. 5. Simplified illustration of the operating principle.

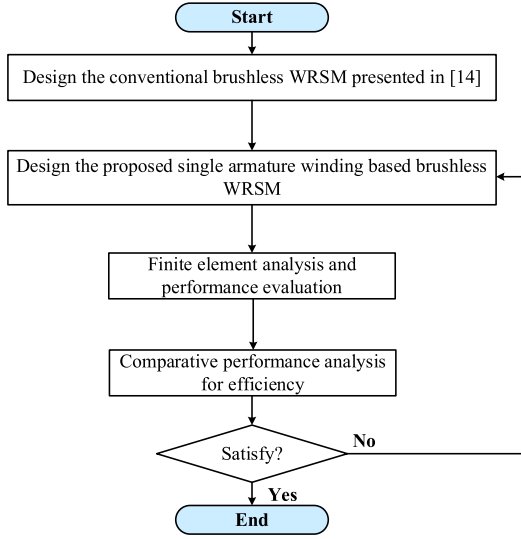


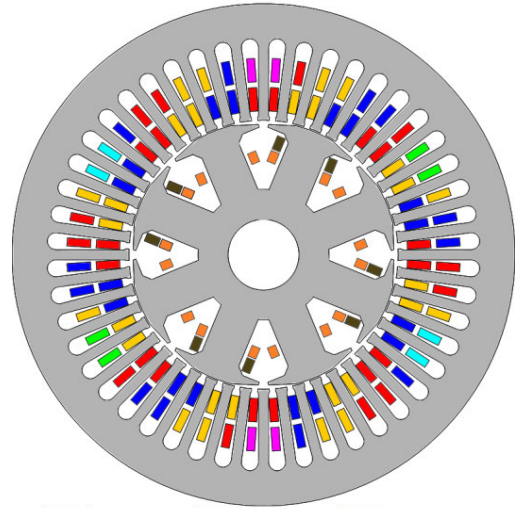
Fig. 6. Design flowchart of the study.

## II. PROPOSED TOPOLOGY AND OPERATING PRINCIPLE

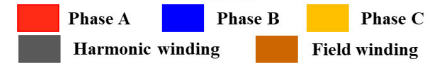
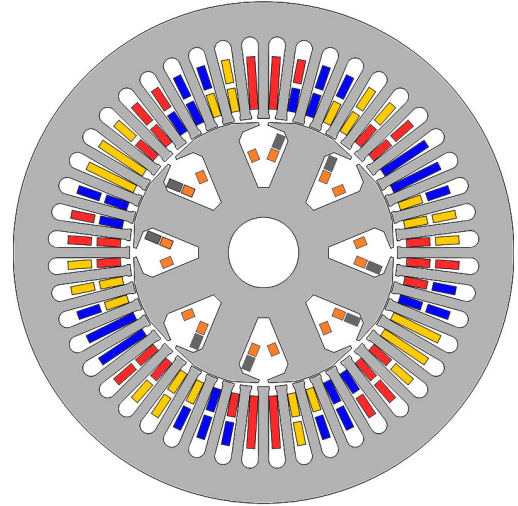
The proposed highly efficient, self-excited brushless WRSM topology employs a novel armature winding configuration that combines single- and double-layer winding arrangements, as shown in Fig. 3. This configuration is designed for a three-phase, eight-pole, forty-eight-slot (8p48s) machine model and is developed using a traditional double-layer winding with a winding factor of 0.933, a coil span of five slots, and a pole pitch of six slots. The winding is then adapted to include a single-layer configuration for four slots per phase, resulting in 12 slots with single-layer and 36 slots with double-layer configuration. The developed winding configuration involves two pole pairs with a double-layer configuration and two pole pairs with a combination of single-layer and double-layer winding arrangements. When the inverter supplies a current of 4 A (peak) per phase, as shown in Fig. 4(a), this new armature winding generates an MMF in the machine's airgap, depicted in Fig. 4(b).

The input armature winding currents are given by

$$\begin{aligned} I_A &= I \cos(\omega t) \\ I_B &= I \cos\left(\omega t - \frac{2\pi}{3}\right) \\ I_C &= I \cos\left(\omega t + \frac{2\pi}{3}\right) \end{aligned} \quad (1)$$



(a)



(b)

Fig. 7. 2-D layout of the (a) conventional and (b) proposed WRSM models.

where  $I$  is the peak phase current and  $\omega$  is the angular frequency.

The fast Fourier transform (FFT) of this MMF reveals both a fundamental component and a suitable sub-harmonic MMF component with an amplitude of around 12.21% of the fundamental. A simplified illustration of these developed airgap flux components is given by

$$F = \frac{3}{2\pi} \left[ N_f I_f \cos(\omega t - \theta) + N_s I_s \cos\left(\frac{\omega t - \theta}{2}\right) \right] \quad (2)$$

where  $I_f$  and  $I_s$  represent the peaks of the fundamental and sub-harmonic current components, respectively.  $N_f$  denotes the number of turns per phase for the pole pairs with a double-layer winding pattern, while  $N_s$  represents the number of winding turns per phase for the pole pairs with a combination of single-layer and double-layer winding

TABLE I  
PARAMETERS OF MACHINE MODELS

Parameter	Conventional Model	Proposed Model
Number of stator slots	48	48
Number of poles	8	8
Stator outer diameter	177.5 mm	177.5 mm
Stator inner diameter	95 mm	95 mm
Rotor outer diameter	94 mm	94 mm
Rotor pole width	14 mm	14 mm
Rotor speed	900 rpm	900 rpm
ABC winding number of turns per phase	30	30
ABC winding resistance	1.65 $\Omega$	1.65 $\Omega$
XYZ winding number of turns per phase	10	-
XYZ winding resistance	0.55 $\Omega$	-
Harmonic winding number of turns	20	20
Harmonic winding resistance	1 $\Omega$	1 $\Omega$
Field winding number of turns	150	150
Field winding resistance	1 $\Omega$	1 $\Omega$
Airgap	0.5 mm	0.5 mm

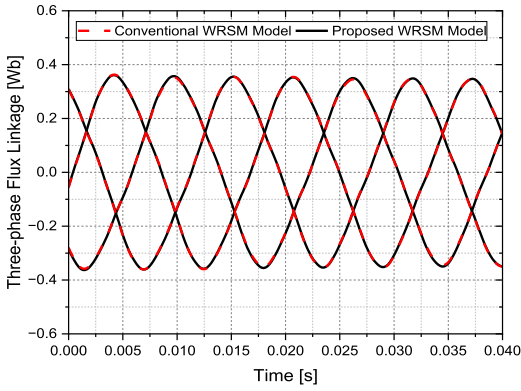


Fig. 8. Flux linkages for the conventional and proposed WRSM models.

arrangements. The variable  $\theta$  corresponds to the rotor angular position.

The rotor of the machine comprises two types of windings: 1) a four-pole harmonic winding and 2) an eight-pole field winding. These windings are connected in series through a full-bridge diode rectifier.

The flux linkage for the harmonic winding can be calculated as follows:

$$\lambda_h = \frac{3N_h}{2\pi} P_g \left[ N_f I_f \cos(\omega t - \theta) + N_s I_s \cos\left(\frac{\omega t - \theta}{2}\right) \right] \quad (3)$$

where  $N_h$  is the harmonic winding number of turns,  $P_g$  is the airgap permeance, and  $\lambda_h$  is the harmonic winding flux linkage.

The sub-harmonic field is not synchronized with the field winding and is captured by the rotor winding with the same number of pole pairs. Neglecting the effect of the fundamental field on the four-pole harmonic winding, the induced voltages can be expressed as follows:

$$e_h = \frac{3N_h}{4\pi} \omega P_g N_s I_s \sin\left(\frac{\omega t - \theta}{2}\right) \quad (4)$$

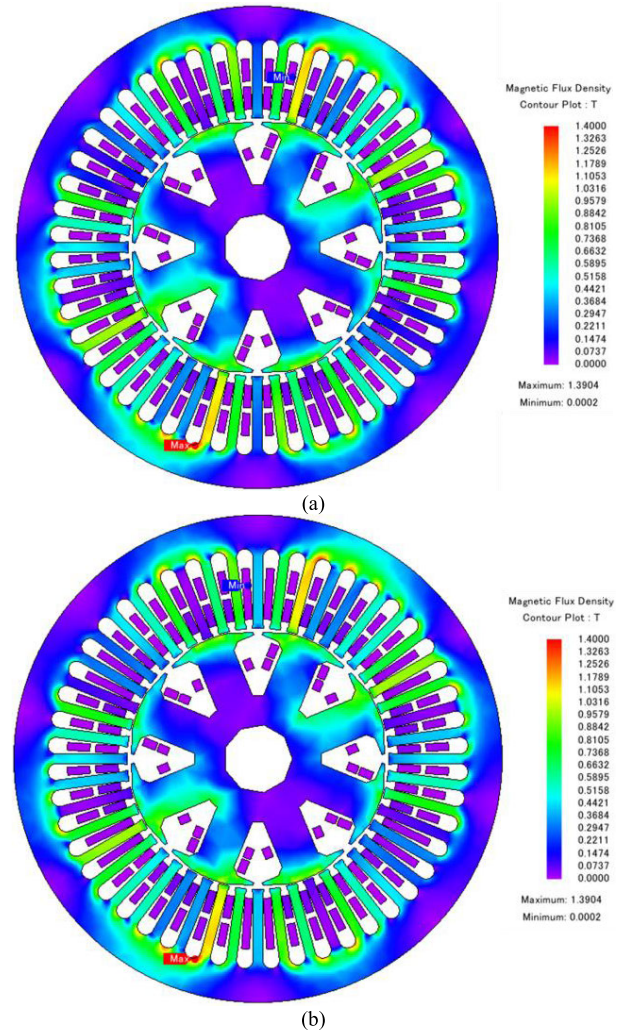


Fig. 9. Flux density distribution plot for the (a) conventional and (b) proposed WRSM models.

where  $e_h$  denotes the induced voltage in the rotor harmonic winding.

These induced voltages are rectified to excite the eight-pole rotor field winding. Equation (4) shows that the magnitudes of the induced harmonic winding and rectified field winding voltages depend on the winding turns of pole pairs having the combination of single-layer and double-layer winding arrangements. Fig. 5 presents a simplified illustration of the operating principle, while the design flowchart of the study is provided in Fig. 6.

### III. ELECTROMAGNETIC ANALYSIS

For the electromagnetic analysis and comparative performance assessment aimed at lowering torque ripple, minimizing losses, and enhancing efficiency, two machine models, shown in Fig. 7(a) and (b), were developed using 2-D finite-element analysis (FEA) in JMAG-Designer version 22.2. The structural parameters of these machines are presented in Table I. The conventional WRSM model includes two serially connected armature windings, named ABC and XYZ, with 30 and 10 turns per phase, respectively. An input armature current of 4 A (peak) per phase, as shown in Fig. 4(a), is supplied to the armature winding of both the conventional and proposed

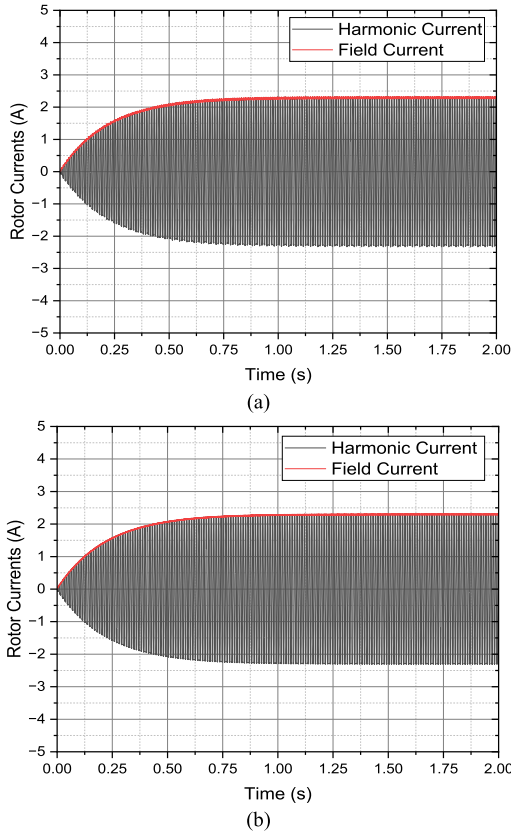


Fig. 10. Rotor currents for the (a) conventional and (b) proposed WRSM models.

brushless WRSM models. These currents generate fundamental and sub-harmonic fields in the machines' air gaps.

Figs. 8 and 9 show the flux linkages and magnetic flux density distribution plots for the conventional and proposed brushless WRSM models, respectively. These figures demonstrate that both models operate under a saturation level of 1.4 T. The four-pole sub-harmonic field induces a harmonic current in the rotor's harmonic winding, which is then rectified to excite the eight-pole rotor field winding.

The induced harmonic and rectified field winding currents for the conventional and proposed brushless WRSM topologies are presented in Fig. 10(a) and (b), respectively. The magnitudes of the induced harmonic and rectified field winding currents are approximately the same for both models: 1.9 A (rms) for the harmonic current and 2.3 A (average) for the rectified field winding current.

The electromagnetic interaction between the main stator and rotor fields generates torque. The developed torque for the conventional and proposed brushless WRSM models is 10.68 and 10.7 nm, with torque ripples of 19.57% and 16.9%, respectively. The output torque of the models is presented in Fig. 11(a) and (b).

To calculate the losses and efficiency of the conventional and proposed WRSM models, a loss study was conducted in JMAG-Designer to evaluate the core losses of both machines. Copper losses were calculated based on the resistance of the windings and the current flowing through them during operation. Fig. 12(a) presents the stator and rotor copper and core losses for both WRSM models, while Fig. 12(b) shows the total losses along with input and output power.

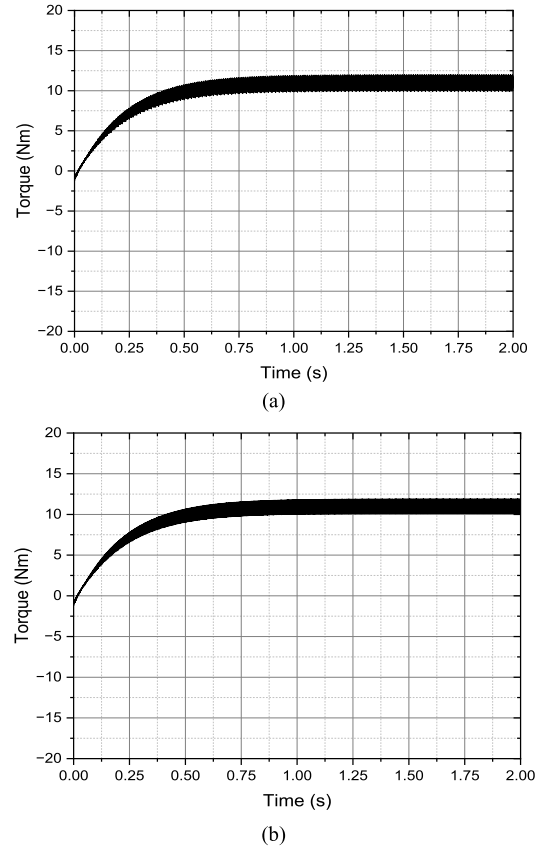


Fig. 11. Output torque for the (a) conventional and (b) proposed WRSM models.

TABLE II  
FEA RESULTS

Parameter	Conventional Model	Proposed Model
RMS harmonic current	1.9 A	1.9 A
Average field current	2.3 A	2.3 A
Average torque	10.68 Nm	10.7 Nm
Torque ripple	19.57%	16.9%
Stator core losses	40.25 W	40.33 W
Rotor core losses	10.57 W	10.78 W
Harmonic winding copper losses	3.57 W	3.57 W
Field winding copper losses	5.25 W	5.25 W
Armature winding copper losses	52.8 W	39.6 W
Total losses	112.46 W	99.56 W
Input power	1119.8 W	1108.3 W
Output power	1007.3 W	1008.7 W
Efficiency	89.96%	91.02%

The results indicate that the stator core losses for the conventional and proposed models are 40.25 and 40.33 W, respectively, while the rotor core losses are 10.57 and 10.78 W, respectively. The stator copper losses for the conventional brushless WRSM model are calculated to be 52.8 W; however, for the proposed topology, the stator copper losses are reduced to 39.6 W which is 13.2 W lower than the conventional topology due to its single-armature winding configuration. Since the harmonic and field winding currents are identical for both models, the harmonic and field winding copper losses are

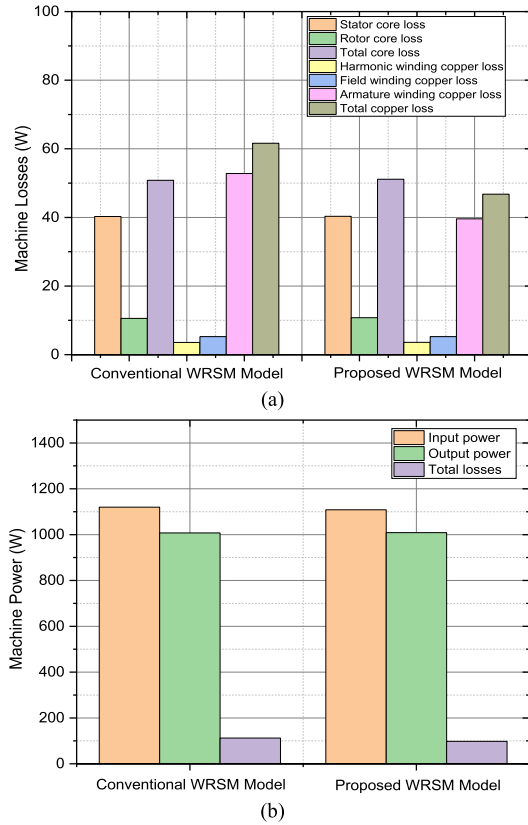


Fig. 12. For the conventional and proposed brushless WRSM models. (a) Stator and rotor core and copper losses. (b) Total input power, output power, and losses.

also the same: 3.57 W for the harmonic winding and 5.25 W for the field winding.

The total input power for the conventional and proposed models is approximately 1119.8 and 1108.3 W, respectively, while the output power for both models is 1007.3 and 1008.7 W, respectively. Based on these results, the efficiency of the conventional topology is calculated to be 89.95%, while the proposed brushless WRSM model achieves an efficiency of 91.1%. These results are further presented in tabular form in Table II.

#### IV. CONCLUSION

In this article, a highly efficient, self-excited topology for the brushless operation of WRSM was proposed. A novel armature winding, combining single- and double-layer configurations, was designed to generate a sub-harmonic MMF component in addition to the fundamental MMF in the machine's air gap. The theory and operation of the machine were validated using 2-D FEA.

The performance of the proposed topology was compared with that of the conventional cost-effective dual-armature winding-based brushless WRSM topology, focusing on torque ripple, losses, and efficiency. These results suggest that the proposed topology offers 2.67% low torque ripple,

11.47% lower losses, and 1.06% higher efficiency compared to the conventional topology, due to its single-armature winding configuration. With its reduced armature winding losses, the proposed topology could serve as a promising alternative for high-power applications.

#### ACKNOWLEDGMENT

This work was supported by the European Commission under the Horizon Europe Marie Skłodowska-Curie Actions call HORIZON-MSCA-2022-PF-01-01-MSCA Postdoctoral Fellowships 2022 under Grant 101108122.

#### REFERENCES

- [1] Y. Amara, L. Vido, M. Gabsi, E. Hoang, A. H. B. Ahmed, and M. Lecrivain, "Hybrid excitation synchronous machines: Energy-efficient solution for vehicles propulsion," *IEEE Trans. Veh. Technol.*, vol. 58, no. 5, pp. 2137–2149, Jun. 2009.
- [2] C. Rossi, D. Casadei, A. Pilati, and M. Marano, "Wound rotor salient pole synchronous machine drive for electric traction," in *Proc. 41st Conf. Rec. IEEE Ind. Appl. Conf. IAS Annu. Meeting*, vol. 3, Tampa, FL, USA, Oct. 2006, pp. 1235–1241, doi: 10.1109/IAS.2006.256689.
- [3] S.-H. Do, B.-H. Lee, H.-Y. Lee, and J.-P. Hong, "Torque ripple reduction of wound rotor synchronous motor using rotor slits," in *Proc. 15th Int. Conf. Elect. Mach. Syst. (ICEMS)*, Oct. 2012, pp. 1–4.
- [4] Q. Ali, S. S. H. Bukhari, and S. Atiq, "Variable-speed, sub-harmonically excited BL-WRSM avoiding unbalanced radial force," *Electr. Eng.*, vol. 101, no. 1, pp. 251–257, Apr. 2019.
- [5] S. S. H. Bukhari, G. J. Sirewal, M. Ayub, and J. Ro, "A new small-scale self-excited wound rotor synchronous motor topology," *IEEE Trans. Magn.*, vol. 57, no. 2, pp. 1–5, Feb. 2021.
- [6] S. S. H. Bukhari, M. A. Shah, J. Rodas, M. Bajaj, and J.-S. Ro, "Novel sub-harmonic-based self-excited brushless wound rotor synchronous machine," *IEEE Can. J. Electr. Comput. Eng.*, vol. 45, no. 4, pp. 365–374, Apr. 2022.
- [7] L. Sun, F. Yao, and X. Gao, "Stator current control method of brushless harmonic excitation synchronous machine," in *Proc. IEEE Conf. Expo Transp. Electrific. Asia-Pacific (ITEC Asia-Pacific)*, Beijing, China, Aug. 2014, pp. 1–4.
- [8] Q. An, X. Gao, F. Yao, L. Sun, and T. Lipo, "The structure optimization of novel harmonic current excited brushless synchronous machines based on open winding pattern," in *Proc. IEEE Energy Convers. Congr. Exposit. (ECCE)*, Pittsburgh, PA, USA, Sep. 2014, pp. 1754–1761.
- [9] L. Sun, X. Gao, F. Yao, Q. An, and T. Lipo, "A new type of harmonic current excited brushless synchronous machine based on an open winding pattern," in *Proc. IEEE Energy Convers. Congr. Expo. (ECCE)*, Pittsburgh, PA, USA, Sep. 2014, pp. 2366–2373.
- [10] F. Yao, Q. An, X. Gao, L. Sun, and T. A. Lipo, "Principle of operation and performance of a synchronous machine employing a new harmonic excitation scheme," *IEEE Trans. Ind. Appl.*, vol. 51, no. 5, pp. 3890–3898, Sep. 2015.
- [11] F. Yao, Q. An, L. Sun, and T. A. Lipo, "Performance investigation of a brushless synchronous machine with additional harmonic field windings," *IEEE Trans. Ind. Electron.*, vol. 63, no. 11, pp. 6756–6766, Nov. 2016.
- [12] F. Yao, D. Sun, L. Sun, and T. A. Lipo, "Dual third-harmonic-current excitation principle of a brushless synchronous machine based on double three-phase armature windings," in *Proc. 22nd Int. Conf. Electr. Mach. Syst. (ICEMS)*, Harbin, China, Aug. 2019, pp. 1–4.
- [13] Q. Ali, T. A. Lipo, and B. Kwon, "Design and analysis of a novel brushless wound rotor synchronous machine," *IEEE Trans. Magn.*, vol. 51, no. 11, pp. 1–4, Nov. 2015.
- [14] G. J. Sirewal and S. S. H. Bukhari, "Cost-effective scheme for a brushless wound rotor synchronous machine," *World Electric Vehicle J.*, vol. 12, no. 4, p. 194, Oct. 2021.